PENG SIMIN, SHI GANG, CAO YUNFENG CAI XU

Wind Power Research Center & State Key Laboratory of Ocean Engineering, Shanghai Jiao Tong University

Control of different-rating battery energy storage system interface to a microgrid

Abstract. *This paper focuses on different-rating battery energy storage system (BESS) integrated into a microgrid. To improve the power quality and satisfy the requirements of power system, it is necessary to integrate different-rating BESS composed battery modules (BM) and power conditioning system (PCS) into the microgrid. The BESSs can supply suddenly changed loads, especially for sensitive loads that must have uninterruptible power supply. A new control strategy included slack mode control and load mode control is presented to enable the BESSs operate in two operation mode: the free-slack operation mode and the load-sharing operation mode. In the load sharing operation mode,the controller enable various load proportionally shared by two different-rating BESS parallelly operating without communication between them In the free-slack mode operation, the BESSs acting as a free-slack can adequately balance the active and reactive power of the microgrid to maintain the voltage and frequency at point of common coupling (PCC) to a desired level. The advantage of the proposed control method is that the unified controller is employed for the two operation mode without swithing between different controllers. Details of modeling of the BM and PCS and the corresponding control strategy are described. The effectiveness of the BESSs and proposed control method is verified through simulations and experiments.*

Streszczenie. *W artykule omówiono bateryjny system gromadzenia energii BESS zintegrowany w mikrosiecią. W celu poprawy jakości energii łączy się systemy BESS z układami kondycjonowania PCS. System BESS działający jako układ zabezpieczający przed chwilowymi zanikami energii musi cechować się niezawodnością. Zaprezentowano nowa strategię sterowania łączącą tryb łagodny i tryb kontroli obciążenia. Zaletą metody jest że do sterowania stosowany jest zunifikowany kontroler bez potrzeby przełączania między różnymi kontrolerami. Skuteczność c metody potwierdziły symulacje i eksperymenty. (**Sterowanie systemem bateryjnego gromadzenia energii współpracującym z mikrosiecią**)*

Keywords: battery energy storage system, unified controller, load proportionally sharing, voltage and frequency control, power system stability.
Słowa kluczowe: bateryjny system gromadzenia energii, kontrola napięcia I częstotliwości, stabilność system zasilania.

1. Introduction

With the development of economy and power electronic technology, high penetration of distributed generation (DG) using renewable energy such as wind and solar energy has been considered as a solution for economical and environmental issues of conventional power system. Due to the rapid proliferation of distributed resource (DR) in the DG which may lead to some problems as it solves, a promising concept of a microgrid has been brought about, which views the DR and associated loads as a subsystem [1][2]. The microgrid employs an advanced method which enables integrating an infinite number of DRs with the electricity grid, without changing the structure of exiting power system. The microgrid will separate from the utility and into islanded mode of operation when there are large events like voltage collapses or disturbances in the utility, and intentionally reconnect to the utility while the faults are no longer present.

It is well known that the power delivered by the DG composed of DRs such as wind energy is not stable and fluctuates. And disturbances like load perturbation have adverse effects on frequency at PCC (f_{PCC}) and voltage at PCC (V_{PCC}) when the microgrid connects to the utility grid, especially in islanded operation in a power system with high penetration of wind power generation. Moreover, for safe operation of any sensitive devices in the microgrid, it is not desirable to have any sudden change in the f_{PCC} and V_{PCC} . As a promising solution, the battery storage technologies can play a vital role in maintaining the voltage and frequency within an acceptable level [3-7]. In [3], a battery energy storage is directly connected in parallel with the DC link of the back-to-back PWM converter of the DFIG to maitain system stablity. By theoretical analysis, a DC storage module is indirectly connected to the DC bus of the power electronic interface of each DR through a DC-DC converter, which decouples dynamics of DR from those of the microgrid[4][5]. A new strategy[6] for the control of the f_{PCC} and V_{PCC} , a self-excited induction generator based wind generator is investigated, which uses only a voltage feedback loop to control the voltage and frequency of the DR. The control strategies presented above can maintain the system stability, but the BESS is used as a supplement coordinating with the DRs ,not acting as a free-slack to regulating the f_{PCC} and V_{PCC} .

At the same time, the BESSs with different rating are parallelly operated to meet the demand of increased electrical loads, and the major problem of good sharing the active and reactive power in parallel-operated BESSs comes into consideration. Many control methods have been investigated extensively in parallel converters for linear/nonlinear loads[2][8-11]. A new method[2] based on traditional droop characteristics is investigated by H.Lasseter to keep the DRs to operate in parallel to the grid or operate in island,however, the DGs must be dispatchable. A controller was developed to share nonlinear loads by adjusting the output voltage bandwidth with the delivered harmonic current in [8]. Taking into account that the line impedance is mainly resistive in low frequency microgrid,a load sharing controller for islanding parallel inverters in an ac-distributed system is proposed[10]. The control methods described above are too complicated to realize in the digital processor, and another controller or DGs must be added into the system to maintain the system stability.

In this paper, A new control strategy included slack mode control and load mode control is presented to enable the BESSs operate in two operation mode: the free-slack operation mode and the load-sharing operation mode. In the load sharing operation mode, the controller enable various load proportionally shared by two various rating BESS parallelly operating without communication between them, only using local measurements of the BESS to demonstrates the plug-and-play feature of the BESSs regardless of the type of battery In the free-slack mode operation, the BESSs acting as a free-slack can adequately regulate the active and reactive power of the microgrid to maintain the f_{PCC} and V_{PCC} to a desired value. This enable the system to have the ability of supply the various loads, especailly sensitive loads The advantage

of the proposed control method is that the unified controller is employed for the two operation mode without swithing between different controllers. Moreover, it simplifies the controller implementation and optimization and contribute to the decrease of the total investment of the microgrid.

2. System Configuration and Operation

Figure 1 shows a simple scheme of a microgrid that consists of a combination of two-parallel-operated BESS, distributed loads, a static breaker (SB), and a DR. Each BESS composes a battery module and a PCS which can transfer energy to the local ac bus. The PCS based on voltage and frequency (VF) controller couples the BM to the PCC through a delta-wye transformer, acting as a source of leading or lagging active/reactive current. The microgrid can be connected to the utility (V_s) through the SB at the PCC. The DR is mainly used to provide the power absorbed by the BM during its charge period. The distributed loads incorporate a large motor and a sensitive load(SL).

After islanding, the utility grid is not present, and the parallel-operated BESSs should be able to share the instantaneous power difference between the load and the DR like DFIG during fast load changes or/and wind fluctuates. Each BESS should maintain the voltage and frequency at the PCC using only local information. The PCS can not only convert the input dc voltage to a three-phase voltage with desired magnitude, frequency and phase angle at the PCC, but also supply bidirectional controllable active and reactive power to limit the fluctuation of the f_{PCC} and V_{PCC} to an allowable range. The BM is activated when the distributed loads start, and provides the instantaneous power difference between the load and the DR.

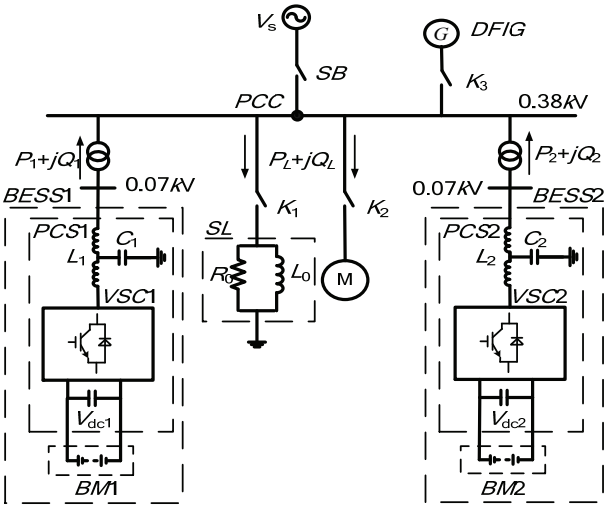

Fig.1 Schematic diagram of a microgrid

3. System Model and Control Strategy

Figure.2 shows the control scheme of a BESS with two close-loop control, voltage control loop and frequency control loop respectively. The measured line voltage (V_{ab} and V_{bc}) and phase current (i_a, i_b and i_c) are sent to the calculator, and yield real-time values of the converter output real and reactive power (P, Q) and the measured voltage amplitude V_m at PCC. The slack mode control is implemented to generate required frequency ω_s and required voltage amplitude V_s respectively, and the load mode control based on the traditional droop characteristics is used to generate load frequency ω_L and load voltage amplitude V_L respectively. The error of V_s and V_L is given as input to a PI controller of voltage closed loop to generate the modulation index m ,and the error of ω_s and ω_L is given as input to a PI controller of frequency closed loop to generate the modulation index m . The ω and m are sent to PWM pulse generator to issue correct switching signals for the converter tracking the requested voltage magnitude and frequency.

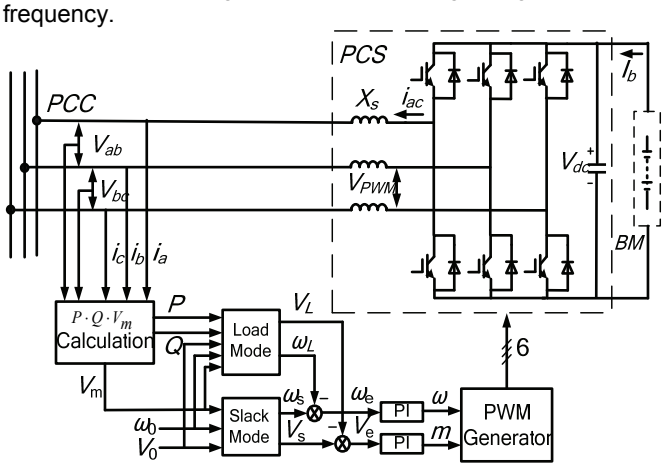

Fig.2 Schematic diagram of control scheme for a BESS with two close-loop control

3.1 Battery Model and Control Method

For modeling the BM, well-known Thevenin equivalent circuit of the battery model is used [12], shown in Fig. 3. It takes into consideration the nonlinear characteristics of battery element depending on the temperature and SOC during charging and discharging cycle as same as the internal resistance.

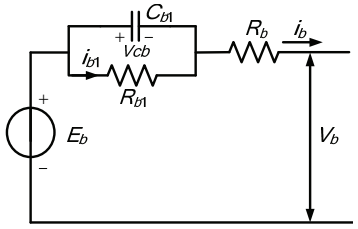

Fig.3 Model of the battery

The battery side current and its internal voltage derivative can be given as

$$\begin{cases} i_b = \dfrac{(V_b - V_{cb} - E_b)}{R_b} \\ C\,\dfrac{dV_{cb}}{dt} = i_b - \dfrac{V_{cb}}{R_{b1}} \end{cases} \tag{1}$$

where E_b is the battery open circuit voltage, V_{cb} is the voltage across capacitor C_{b1}, V_b is the terminal voltage of the battery and R_b is the internal resistance of the battery and R_{b1} is the charge/discharge resistance of the battery. The parameters of the nonlinear systems are dependent on empirically determined constants which can be defined as [13]:

$$\begin{cases} E_b = E_{b0} - K(273+\theta)(1-SOC) \\ R_0 = R_{00} + A(1-SOC) \\ R_{b1} = -R_{b0}\ln(DOC) \\ \tau = R_{b1} * C_{b1} \end{cases} \tag{2}$$

where E_{b0}, K, R_{00}, A, R_{b0}, τ are constants for a particular battery. SOC and DOC are sued to quantify the level of charge of the battery.

The BM plays a major role for regulating the voltage and frequency at PCC to the acceptable level, and the stored or released power of the BM at time t can be presented as follows:

(3) $$P_b(t) = [P_D(t) - P_L(t)] / \eta$$

where $P_b(t)$ is the stored or released energy of the BM at times t, $P_D(t)$ is the total active power generated by the DFIG at time t and $P_L(t)$ is the total active power consumed by the linear/nonlinear loads at time t, η is the charging / discharging efficiency of the BM depending on the charging /discharging current.

If $P_D(t) > P_L(t)$, the BM will be under charging mode until the BM is fully charged. If $P_D(t) = P_L(t)$, the BM just remains the voltage and frequency at PCC to an acceptable level, not storing or releasing any power. If $P_D(t) < P_L(t)$, the BM will be under discharging mode and start to discharge, especially, supplying solely the loads for several hours when the wind turbines is shutdown.

3.2 PCS and Operation Mode

PCS is a major part of the BESS, which interfaces the BM to the loads (utility/end user) and regulates the battery charge/discharge rate, power flow, etc. The schematic diagram of the PCS studied in this paper is shown in Fig. 2. The PCS makes VSC run in four-quadrant of the P-Q plane by regulating the value of the modulation index m of the converter and phase angle δ, between the fundamental component of the converter output voltage V_{PWM} and voltage at the PCC. The P and Q equations are represented respectively [14][15]:

(4) $$P = \frac{V_{PCC} V_{dc}}{\omega L} m \sin\delta$$

(5) $$Q = \frac{V_{PCC}}{\omega L}(V_{PCC} - m V_{dc} \cos\delta)$$

Assuming a lossless system, the output power of the BM must be equal to the output power of the PCS and they can be expressed by

(6) $$P = \frac{V_{PCC} V_{dc}}{\omega L} m \sin\delta = P_b = V_{dc} I_b$$

where I_b is the DC current of the BM. If the BM is under discharging mode, I_b is positive. As shown in equation (4). (5) and equation (6), the P and P_b is proportion to δ and Q is proportion to m, that is, P and P_b is primarily controlled by the angle δ while Q is regulated by the value of m. And the I_b is easily regulated by the value of δ to achieve the required load sharing performance due to the V_{dc} is almost constant.

3.3 Proposed Control Scheme

In the islanding mode, the main objective of the system is to maintain the f_{PCC} and V_{PCC} constant under any perturbations and to feed the different loads, especially the sensitive loads. In this paper, a new method based two-close-loop control is presented, which comprises mainly two parts: slack mode control and load mode control.

3.3.1 Slack mode control

For a microgrid, especially in islanded mode, it is important to maintain the f_{PCC} and V_{PCC} constant under both source and load power perturbations. The slack mode control is used to generate the required voltage magnitude and required frequency, which contributes to the BESS acts as a free-slack in the microgrid. Only a voltage loop is implemented in the slack mode control as shown in Fig.4. A PI compensator regulates the PCC measured voltage V_m to track V_0 and the control laws of the voltage loop may be expressed mathematically as

(7) $$V_s = (k_{sp} + \frac{k_{si}}{s})(V_0 - V_m)$$

where k_{sp} and k_{si} are the proportional and integral gains of the voltage loop PI conpensator. In this paper, no closed loop for the f_{PCC} regulation is utilized due to the frequency control is self-regulatory [15]. The frequency control laws can be expressed mathematically as

(8) $$\omega_s = k\omega_0$$

where k is the frequency ratio.

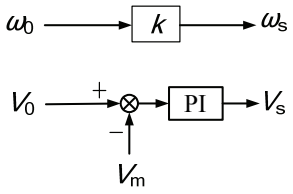

Fig. 4 Slack mode control

3.3.2 Load mode control

As shown in Fig.1, the system consisting of two parallel BESSs operates in the islanding mode. This system can be expanded to multiple parallel BESSs, and the conventional droop characteristics are usually used to these systems. Neglecting the power losses, the power balance within the autonomous operation suggests

(9) $$P_L = P_1 + P_2$$

(10) $$Q_L = Q_1 + Q_2$$

where P_L is the total active power of the loads, Q_L is the total reactive power of the loads.

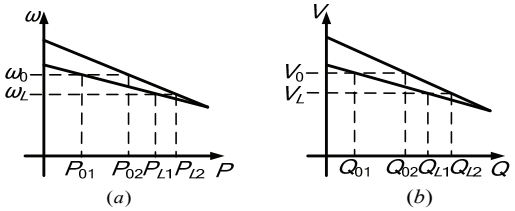

Fig.5 Illustration of the droop control scheme. (a) Frequency droop (b) Voltage droop.

The active power sharing between these two PCSs is determined according to a droop strategy, as shown in Fig.5. the control laws of the droop characteristics can be represented by

(11) $$\omega_L = \omega_0 - k_{\omega i} P_i$$

(12) $$V_L = V_0 - k_{vi} Q_i$$

where V_0 and ω_0 are the voltage amplitude and frequency when the microgrid is grid-connected, i is the i^{th} PCS, and V_L and ω_L are load voltage magnitude and load converter frequency of i^{th} PCS when the microgrid is

islanded. $k_{\omega i}$ and k_{vi} are droop coefficients for ω_L and for V_L respectively .

For parallel operation of the PCSs of different rating, the droop coefficients should be modified depending on their rating:

(13) $$k_{\omega 1} * P_1 = k_{\omega 2} * P_2$$

(14) $$k_{v1} * Q_1 = k_{v2} * Q_2$$

3.3.3 Voltage control loop.

For the PCC voltage regulation, as shown in Fig.2, the value of m is responsible for setting the V_{PCC} and it is processed by a PI controller of the voltage closed loop. The input to the PI controller is the difference between the required voltage magnitude V_s and the load voltage V_L. The control laws of the voltage loop can be presented by

(15) $$m = (k_{mp} + \frac{k_{mi}}{s})(V_s - V_L)$$

where k_{mp} and k_{mi} are the proportional and integral controller gain constants.

3.3.4 Frequency control loop.

As shown in Fig.2, the value of ω is responsible for setting the f_{PCC} and it is processed by a PI controller of the frequency closed loop. The input to the PI controller is the difference between the required frequency magnitude ω_s and the load frequency ω_L. The control laws of the frequency loop can be given by

(16) $$\omega = (k_{\omega p} + \frac{k_{\omega i}}{s})(\omega_s - \omega_L)$$

where $k_{\omega p}$ and $k_{\omega i}$ are the proportional and integral controller gain constants.

4. Simulation Results

To verify the effectiveness of the proposed control strategy for two parallel operated BESSs, comprehensive simulation study is carried out with different types of loads for the system shown in Fig.1 during islanded mode. Two types of load are investigated here-SL and motor load. The system simulation parameters used are listed in Table1, given in Appendix. And the simulation is carried out in the environment of PSCAD/EMTDC. Dynamic response of the system to load changes is shown in Fig.6-7.

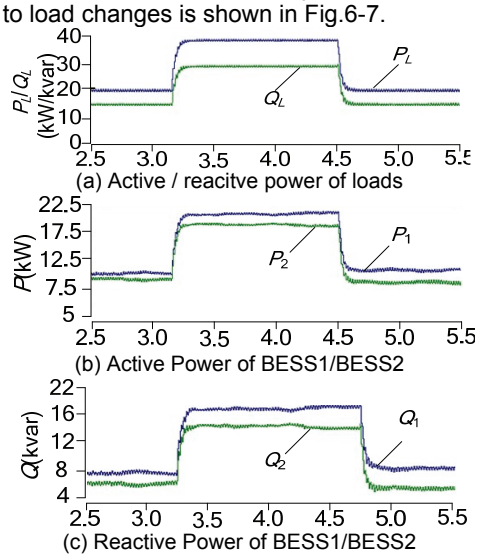

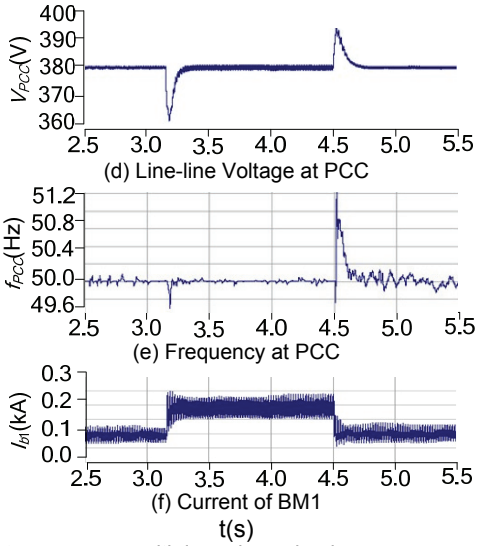

Fig.6 System response with impedance load

Fig.6 shows the response of the parallel operated BESS with the impedance load changing. Initially, the system is operating in steady-state and delivers 20+j15kVA power to the load. At 3.2s the SL is increased to 40+j30kVA,. The load is reduced back to its nominal value at 4.5s. Fig.6 (a) shows the active and reactive power drawn by the load having a step increase at 3.2s and a step decrease at 4.5s. Fig. 6(b) and (c) illustrate the changes of active and reactive power of BESS1/BESS2 respectively. It can be seen that BEES1 shares more loads than BESS2 in accordance with their droop characteristics. Fig. 6(d) shows the changes of the V_{PCC} for the conditions corresponding to the variation of the reactive power. The voltage reduces immediately in accordance with the increase of reactive power of load, and restores to rated value within a few seconds (0.1s) for the absorbed power is compensated by the BESS. Fig. 6(e) illustrates the changes of the f_{PCC} that is controlled by the parallel operated BESS. The active power and frequency values are coupled through the power-frequency droop characteristics. The f_{PCC} suddenly falls to 49.6Hz according to the quick increase of active power of the loads,and fast restore to the desired value due to the increase of active power output of the BM Fig. 6(f) shows the step changes of the discharge current of BM of BESS1.

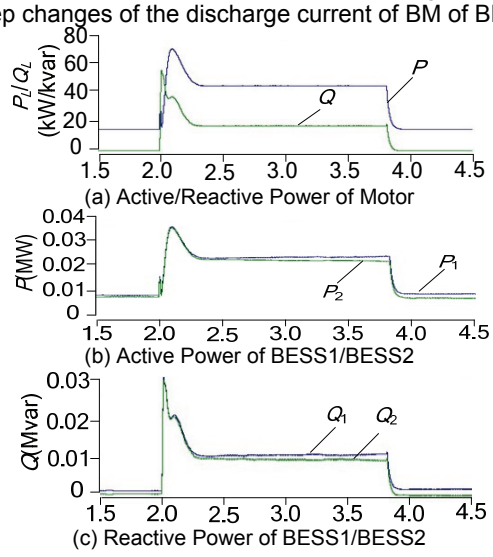

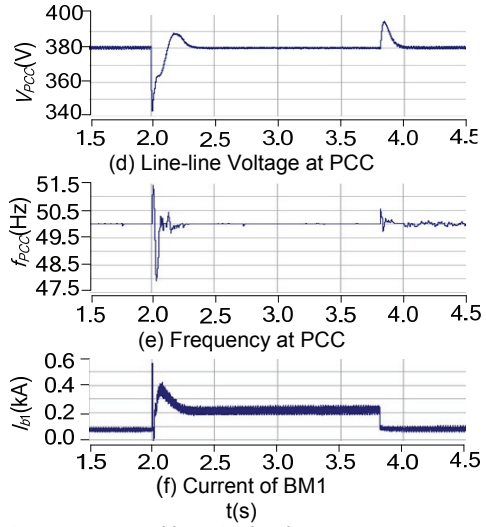

Fig.7 System response with motor load

Fig.7 shows dynamic response of the parallel operated BESS to the motor load. Fig.7 (a), the motor output power, and Fig. 7(b) and (c), the active power and reactive power of BESS1/BESS2, illustrate that the parallel operated BESSs pick up the motor load and share the load proportionally as deserved. For the inertial load, the power drawn by the motor overshoot the normal value at start moment and restore to normal value a few seconds later as shown in Fig.7(a). Corresponding to the variation of motor loads, the output active and reactive power of the BESSs increase sharply and restore to nornal value as shown in Fig.7(b) and (c). To catch up with the sudden power variations of the loads, both of the BESSs increase the output power while the loads increase and decrease the output power according to the fall of the loads. Fig. 7 (d) and (e) show that the f_{PCC} and V_{PCC} restore to the rated value within a short time (0.3s) due to the balance of power flow by the parallel operated BESS during the transients. Fig. 7(f) shows the step changes of the discharge current of BM1 in accordance with the motor load.

5.Experiments Results

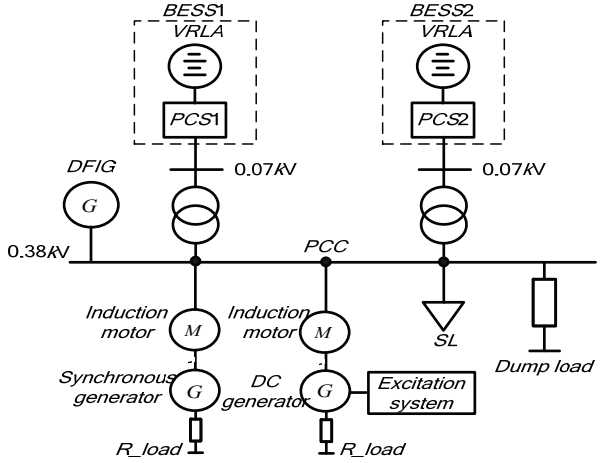

Fig.8 Configuration diagram of experimental setup

An experimental setup for a tested microgird system was fabricated as the diagram shown in Fig.8. System parameters are listed in Table.2, given in Appendix. The test system consists of two parallel connected BESSs of different rating. The comprehensive loads consist of a large induction motor (15kW), a squirrel-cage motor (5.5kW) and SL load. The control strategy was developed by using the DSP processor TM320F2812. Fig.9 shows the photograph of the experimental platform.

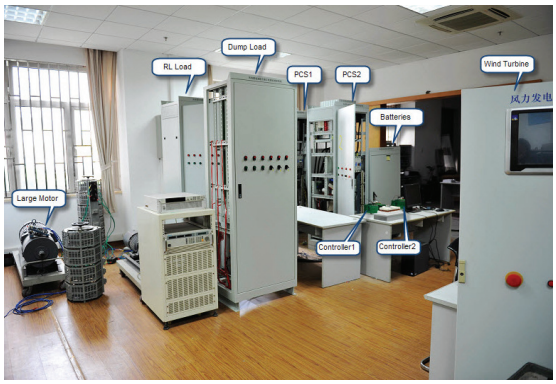

Fig.9 Photograph of experimental setup

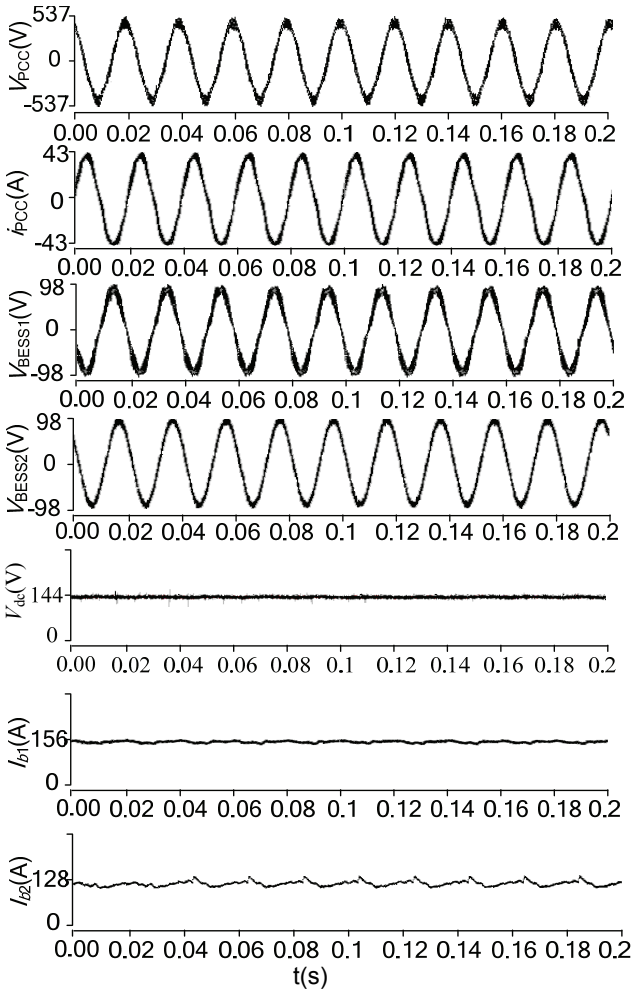

Fig.10 system response to SL load

Fig. 10 illustrates the experimental results of sharing power by two BESSs of different rating when connected to SL load at steady state. As shown in the 1th plot and 2th plot, the V_{PCC} almost maintains at desired nominal value (380V), and its frequency at desired nominal value (50Hz), which means the BESSs can keep the islanded system stablity and support the loads under the load perturbation. Moreover, the output voltage of BESS2 can well track the command nominal value (70V) and the output current at PCC (i_{PCC})can follows the total loads variations, which indicating successful elimination of steady state error by the

use of the proposed controller in the voltage loop. In the 5th plot, the capacitor voltage of BESS1 has a near constant voltage magnitude (144V) without significant variations, similar to the voltage of the BESS2, which means the output power value of the BM in proportion to the output current value of the BM. Namely, the value of the sharing power by two BESSs in parallel is equivalent to the value of the sharing current. In the 6th and 7th plot, the average output current of batteries of BESS1 (I_{b1}) varies proportional to the average output current of batteries of BESS2 (I_{b2}), which presents that the BESSs jointly pick up the SL load demand and share proportionally it as desired.

The experimental results of sharing power by two BESSs in parallel when connected to a large motor of rating 15kW and an induction motor of rating 5.5kW at steady state as shown in Fig. 11. in the 1th plot, the waveforms of the V_{PCC} and i_{PCC} also maintain at the desired value respectively under motor loads in the steady state. And the I_{b1} and the I_{b2} are almost kept to the proportional value of 0.8(67A/85A) to jointly pick up the motor loads based on the same droop characteristics. Moreover, the current direction indicates that two parallel operated BESSs are injecting power flow to the PCC (positive).

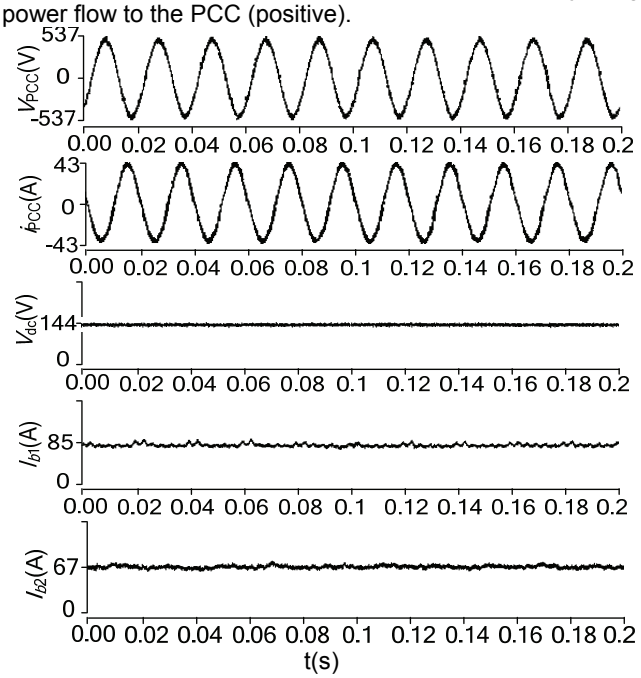

Fig.11 system response to large motor load

6.Discussion

Simulation and experiment results for the system responses shown in Fig.6, Fig.7 and Fig.9, Fig.10 can be summarized as follows.

1) Load sharing proportionally characteristics: According to the profiles P_1 and P_2 shown in Fig.6(b) and Fig.7(b), the P_1 is always proportional to the P_2 based on the droop characteristics, tracking respectively the step changes of the loads. And the sum of the P_1 and P_2 is almost equal to the demand power of the loads, meaning the BESSs can effectively meet the sudden variation of the loads. At the same time, the waveforms I_{b1} shown in Fig.6(f) and Fig.7(f) change corresponding to the variation of the power, and the value of the I_{b1} is always proporational to the value of the and I_{b2} in the 6th and 7th plot of Fig.10 and in the 4th and 5th plot of Fig.11, respectively. Those plots clearly illustrates the excellent load sharing characteristics of the proposed control for the microgrid in the load sharing operation mode.

2) Good control performance: As shown in Fig.6(d) and Fig.7(d), the V_{PCC} can rapidly restore to the rated value in 0.1s and 0.3s, respectively, under RL load and motor load. And the f_{PCC} can also promtly recover to the normal level in a few seconds. Moreover, the waveform of V_{dc} shown in the 5th plot of Fig.10 and the 3th plot of Fig.11 can be maintained at the rated level in spite of the variation of the loads. And although the plot of the f_{PCC} and V_{PCC} shown in Fig.6 and in Fig.7 has obvious change, both of them can still be rapidly regulated to the rated level. Those plots distinctly demomstrate the outstanding balance of the active power and reactive power to maintain the V_{PCC} and f_{PCC} to desired level in the free-slalck operation mode.

3) Power quality of power supply: The small deviation of the V_{PCC} and f_{PCC} can both satisfy the basic power quality requirements of the microgrid in islanded mode to supply the different loads. The experiment waveforms of the V_{PCC} and f_{PCC} shown in Fig.10 and in Fig.11 well testify the effectiveness of the control methods

4) plug-and-play feature: Due to the proposed controller use local measurements of the BESS, there is no communicaiton between each other which provide the plug-and-play feature of the BESS regardless of the battery type.

7. Conclusions

In this paper, a unified controller based on slack mode control and load mode control is presented, which integrates the different rating BESSs connected in parallel into the microgrid. And, to verify effectiveness of the interface and proposed control method, comprehensive simulation study and an experimental setup are carried out. The results show that the proposed controller can rapidly tracks the variations of the various loads when the microgrid in the islanded mode, and the different rating BESSs acting as a free-slack can share proportionally the active power and reactive power to automatically regulate the voltage and frequency at PCC to desired value in spite of the load distrurbance. Moreover, without communication between each other, the controller can provide the plug-and-play feature of BESSs regardless of the type of battery.

Appendix

Table.1 Simulation parameters

System Quantities	Values	
System Frequency (ω_0)	100 π rad/s	
System Voltage(V_0)	0.38kV rms (L-L)	
	BESS1	BESS2
PCS rating	75kVA/50kW	50kVA/40kW
DC voltage(V_{dc})	128V	128V
Inductance (L)	0.04 μH	0.04 μH
Filter Capacitance(C)	66 μF	66 μF
Frequency droop coefficient (k_ω)	0.33Rad/s/kW	0.45Rad/s/kW
Voltage droop coefficient (k_v)	0.033kV/kVAr	0.05kV/kVAr
Transformer rating	380/70V, 80kVA Y/△	
SL load	$40+j30$kVA	
VRLA battery	192Ah,128V,R=0.02 Ω	

Table.2 Experiment parameters

System Quantities	Values	
System Frequency (ω_0)	100 π rad/s	
System Voltage(V_0)	0.38kV rms (L-L)	
PCS rating	BESS1 75kVA/50kW	BESS2 50kVA/40kW
DC voltage(V_{dc})	144V	144V
Inductance (L)	0.04 μH	0.04 μH
Filter Capacitance(C)	66 μF	66 μF
Frequency droop coefficient (k_ω)	0.4Rad/s/kW	0.55Rad/s/kW
Voltage droop coefficient (k_v)	0.5kV/kVAr	0.6kV/kVAr
SL load	$40+j30$kVA	
VRLA battery	240Ah,144V,R=0.024 Ω	

Acknowledgements

This work is supported by the Chinese Key Laboratory Foundation (No. AE010803);Shanghai Science Foundation (No. 08DZ1200504 & No. 08DZ2210502)

REFERENCES

[1] Lasseter,R.H. "MicroGrids," In 2002 Power Engineering Society Winter Meeting, New York, USA, pp.305-308, January 2002.

[2] Piagi,P., Lasseter,R.H."Autonomous control of microgrids," In 2006 Power Engineering Society General Meeting, Montreal, Canada, pp. 496-503, June 2006.

[3] Yazdani,A. "Islanded operation of a doubly-fed induction generator (DFIG) wind-power system with integrated energy storage," Proc. IEEE Canada. Electrical power conference., pp. 1-7, Oct 2007.

[4] Nikkhajoei,H., Lasseter.R.H. " Distributed Generation Interface to the CERTS Microgrid," IEEE Trans. Power Delivery., vol.24, no.3,pp. 1598-1608, July 2009.

[5] Wang L., Lee D.J. " load tracking performance of an autonomous SOFC based hybrid power generation energy storage system, " IEEE trans. energy convers., vol.25,no.1,pp. 128-139, 2010.

[6] Perumal,B.V., Chatterjee,J.K. " Voltage and frequency control of a stand alone brushless wind electric generation using generalized impedance controller, " IEEE Trans .Energy Conversion., vol.23,no.2,pp .632-641, June 2008.

[7] .Stefania,C., Andrea,M.G., Salvatore,R. " Local control of photovoltaic distributed generation for voltage regulation in LV distribution networks and simulation tools," European Transaction on Electrical power., vol.19, no.16,pp.798-813, sept 2009.

[8] Borup,U., Blaabjerg,F., Enjet,P.N. " Sharing of nonlinear load in parallel-connected three-phase converters," IEEE Trans. Ind. Appli., vol.37,no.6,pp. 1817-1823, Nov 2001.

[9] Singh,B., Kasal,G., Chandra A, etc. " Battery based voltage and frequency controller for parallel operated isolated asynchronous generators," In 2007 IEEE International Symposium on Industrial Electronics, Proceedings, Vigo,Spain, pp. 883-888, June 2007.

[10] Guerrero,J.M., Matas,J , de Vicuna,L.G, etc. " Decentralized control for parallel operation of distributed generation inverters using resistive output impedance," IEEE Trans.Ind. Electron., vol.54,no.2, pp. 994-1004, Apirl 2007.

[11] Katiraei,F,, Iravani,M,R. " Power management strategies for a microgrid with multiple distributed generation units," IEEE Trans. Power Systems., vol.21,no.4, pp. 1821-1831, Nov 2006.

[12] Jackey R.A. "A Simple, Effective Lead-Acid Battery Modeling Process for Electrical System Component Selection'. SAE Paper 2007-01-0778., SAE International, Warrendale, PA, 2007.

[13] Ceraolo,M. " New dynamical models of lead-acid batteries'. IEEE trans. power syst., 2000,vol.15,no.4, pp 1184-1190.

[14] Aboul-Seoud,T,, Jatskevich,J. " Improving power quality in remote wind energy systems using battery storage," In 2008 Canadian Conference on Electrical and Computer Engineering, Ontario, Canada , pp. 1668-1671, May 2008.

[15] Shi,G. Cao, Y.F. Li, Z. Cai,X. "Impact of Wind-Battery Hybrid Generation on Isolated Power System Stability," SPEEDAM, Pisa Italy, pp. 757-761, Jun 2010.

Authors: PENG SIMIN, SHI GANG, CAO YUNFENG CAI XU, Wind Power Research Center & State Key Laboratory of Ocean Engineering, Shanghai Jiao Tong University
e-mail: psm1004@sjtu.edu.cn